Relaxin 2 Is Functional at the Ocular Surface and Promotes Corneal Wound Healing

Ulrike Hampel,[1] *Thomas Klonisch,*[2–4] *Eugenia Makrantonaki,*[7] *Saadettin Sel,*[5] *Ute Schulze,*[6] *Fabian Garreis,*[1] *Holger Seltmann,*[7] *Christos C. Zouboulis,*[7] *and Friedrich P. Paulsen*[1]

Purpose. We aimed to determine if the insulin-like peptide hormone relaxin 2 (RLN2) is expressed at the ocular surface and in tears and if RLN2 influences wound healing at the ocular surface, which is associated with extracellular matrix (ECM) remodeling.

Methods. We analyzed transcript levels of human RLN2 and its cognate relaxin-like receptors RXFP1 and RXFP2 in tissues of the ocular surface, lacrimal apparatus, and human corneal (HCE), conjunctival (HCjE) and sebaceous (SC) cell lines. We analyzed effects of human RLN2 on cell proliferation and migration and quantified mRNA expression of matrix metalloproteinases (MMPs) and tissue inhibitors of metalloproteinases (TIMPs) in HCE, HCjE, and SC. Using an alkali-induced corneal wounding model, we analyzed the wound healing rate in C57BL/6 mice eyes after topically applied RLN2.

Results. The presence of RLN2, RXFP1, and RXFP2 transcripts was detected in lacrimal gland, eyelid, conjunctiva, cornea, primary corneal fibroblasts, nasolacrimal ducts, and all three cell lines. ELISA revealed RLN2 protein in all ocular surface tissues analyzed and in human tears. Stimulation of HCE, HCjE, and SC with RLN2 significantly increased cell proliferation and migration. Relative mRNA expression levels of MMP2, MMP9, TIMP1, and TIMP2 were significantly influenced by RLN2 in all three cell lines at different time points studied. The local application of RLN2 onto denuded corneal surface resulted in significantly elevated corneal wound healing.

Conclusions. Our data support a novel role for the RLN2 ligand–receptor system at the ocular surface and in the lacrimal apparatus as a potential future therapeutic during wound healing at the ocular surface. (*Invest Ophthalmol Vis Sci.* 2012; 53:7780–7790) DOI:10.1167/iovs.12-10714

From the Departments of [1]Anatomy II and [5]Ophthalmology, Friedrich Alexander University of Erlangen-Nürnberg, Erlangen, Germany; the Departments of [2]Human Anatomy and Cell Science, [3]Medical Microbiology and Infectious Diseases, and [4]Surgery, University of Manitoba, Winnipeg, Manitoba, Canada; the [6]Department of Anatomy and Cell Biology, Martin Luther University Halle-Wittenberg, Halle/Saale, Germany; and the [7]Departments of Dermatology, Venereology, Allergology, and Immunology, Dessau Medical Center, Dessau-Rosslau, Germany.

Supported by the Natural Science and Engineering Research Council of Canada (TK), Deutsche Forschungsgemeinschaft Grants PA738/6-1 and PA738/1-5, BMBF Wilhelm Roux Program Grant 17/24, and Sicca Forschungsförderung of the Association of German Ophthalmologists.

Submitted for publication August 6, 2012; revised September 6 and October 18, 2012; accepted October 18, 2012.

Disclosure: **U. Hampel**, None; **T. Klonisch**, None; **E. Makrantonaki**, None; **S. Sel**, None; **U. Schulze**, None; **F. Garreis**, None; **H. Seltmann**, None; **C.C. Zouboulis**, P; **F.P. Paulsen**, None

Corresponding author: Ulrike Hampel, Department of Anatomy, Friedrich Alexander University Erlangen-Nürnberg, Faculty of Medicine, Universitätsstraße 19, D-91054 Erlangen, Germany; ulrike.hampel@anatomie2.med.uni-erlangen.de.

Injuries of the ocular surface are among the most common problems presenting to the ophthalmologist. These include mechanical lesions, incorrect use of contact lenses, and contaminants causing erosions of the ocular surface.[1] Effective wound healing, including restitution of the physiological barriers and reconstruction of the rigidity and transparency of the cornea, is an essential step in the process of recovery from injury of the cornea or conjunctiva.[1] These complex cellular and extracellular actions are orchestrated by different immunological mediators.

The peptide hormone relaxin 2 (RLN2) has long been known as a pregnancy hormone, but in recent years the importance of the interaction of RLN2 with its cognate receptors RXFP1 (LGR7) and RXFP2 (LGR8)[2,3] in numerous other normal and diseased conditions has been recognized.[4–10] RLN2 influences collagen turnover and increases migration and proliferation.[11–13] It modulates connective tissue composition by induction of matrix metalloproteinases (MMPs) and their physiological antagonists, the tissue inhibitors of metalloproteinases (TIMPs).[9,10,14–16] Human fibroblasts derived from the lower uterine segment respond to RLN2 by increased gene activity and production of MMP1, MMP2, and MMP3, as well as inhibition of TIMP1 production.[10] In renal fibroblasts, RLN2 induces MMP2 and MMP9 expression, and this induction involves inhibition of the SMAD2 pathway.[17]

Under physiological conditions, the turnover of ocular surface tissues is regulated by MMPs and TIMPs, and MMPs/TIMPs are also involved in the remodeling of the ocular surface after injury. Essential for a rapid wound healing is a sufficient proliferation and migration of epithelial cells. The integrity of the ocular surface seems to be influenced by a complex regulation of hormones.[18–20] It is yet unknown whether RLN2 is present at the ocular surface or in the tear film and if it may exert a possible promoting effect on wound healing by its ability to elevate proliferation and migration and to regulate MMPs and TIMPs.

In the present study, we have characterized the expression of RLN2 and its receptors RXFP1 and RXFP2 in tissues of the ocular surface and lacrimal apparatus, in tears, and in cell lines derived from the ocular surface. Moreover, we investigated the role of RLN2 on the proliferation, migration, and MMP/TIMP expression in cultured human corneal epithelial (HCE), conjunctival epithelial (HCjE), and sebaceous (SC) cell lines. Employing a corneal defect mouse model, we identified human recombinant (r) RLN2 as a novel and highly effective endocrine factor capable of enhancing the re-epithelialization of corneal wounds.

Copyright 2012 The Association for Research in Vision and Ophthalmology, Inc.

Downloaded from iovs.arvojournals.org on 06/17/2019

METHODS

Experimental Animals

All animals in the present study were treated in accordance with the ARVO Statement for the Use of Animals in Ophthalmic and Vision Research and the recommendations of the National Institutes of Health Guide for the Care and Use of Laboratory Animals. The experiments had received governmental approval. Ten-week-old female C57BL/6 mice were used for all experiments in this study. The animals were obtained from Harlan Laboratories (Venray, Netherlands) and kept under normal controlled laboratory conditions with a 12-hour light/dark cycle.

Human Tissue, Tears, and Cell Lines

The study was conducted in compliance with institutional review board regulations for human and animal ethics, informed consent regulations, and the provisions of the Declaration of Helsinki. Lacrimal glands, upper eyelids, conjunctivas, corneas, and nasolacrimal ducts (consisting of lacrimal sac and nasolacrimal duct) were obtained from cadavers (3 males, 12 females, age 53–92 years) donated to the Department of Anatomy and Cell Biology, Martin Luther University Halle-Wittenberg, Germany. All tissues used were dissected from the cadavers between 4 and 12 hours postmortem. The epidermis (skin) and the eyelashes were removed from the middle-area upper eyelids. The donors were free of recent trauma, eye and nasal infections, or diseases affecting lacrimal functions. SV-40-transformed human corneal epithelial (HCE) cells,[21] human spontaneously immortalized epithelial cells from normal human conjunctiva (HCjE),[22] and a Simian virus (SV)-40-transformed sebaceous gland cell line (SC)[23] were cultured as monolayers and used for stimulation experiments. The sebaceous gland cell line used in our work and called SC cell line is the sebaceous gland cell line SZ95.

Cell Culture

HCE and HCjE cells (5×10^6) were seeded into 25 cm^2 flasks and cultured in Dulbecco's modified Eagle's medium (DMEM) (DMEM F12; PAA Laboratories GmbH, Pasching, Austria) containing 10% fetal calf serum (FCS; Biochrom AG, Berlin, Germany). SC cells (5×10^6) were seeded into 25 cm^2 flasks and cultured in Sebomed basal medium (Biochrom AG) containing 10% FCS and 0.1 mg/mL recombinant human epithelial growth factor (rhEGF; purity $\geq$97%; Sigma-Aldrich, Steinheim, Germany). At confluency, cells were exposed to different concentrations (100 and 500 ng/mL) of synthetic human RLN2 (purity $\geq$90%; Phoenix Pharmaceuticals, Burlingame, CA) for 6 and 24 hours in serum-free DMEM (HCE, HCjE) or Sebomed basal medium (SC). Cell lines were cultured, and experimental procedures were performed under normoxic conditions (21% O_2, 5% CO_2).

Culture of Primary Corneal Fibroblasts

Scleral rings were obtained from the Department of Ophthalmology, Martin Luther University Halle-Wittenberg, Germany, and preserved in DMEM for transportation. Scleral tissue was removed from the limbus with a scalpel. Once the corneal endothelium and epithelium had been removed, the stromal tissue was cut into pieces, transferred into 25 cm^2 flasks, and cultured in DMEM containing 10% FCS, 50 μg/mL streptomycin, and 50 IU/mL penicillin (both Sigma-Aldrich). Fibroblasts were used for RT-PCR analysis and cell proliferation assays.

RNA Preparation and cDNA Synthesis

For conventional RT-PCR, tissue biopsies of lacrimal gland, conjunctiva, cornea, and nasolacrimal duct were crushed in an agate mortar under liquid nitrogen and then homogenized with a homogenizer (IKA, Staufen, Germany). Total RNA was isolated using RNeasy kit (QIAGEN, Hilden, Germany). Crude RNA was purified with isopropanol and repeated ethanol precipitation, and contaminating DNA was destroyed by digestion with ribonuclease (RNase)-free deoxyribonuclease (DNase) I (30 minutes, 37 C; Boehringer, Mannheim, Germany). Additional incubation with RQ1-RNase-free DNase (Promega, Mannheim, Germany) was conducted on purified RNA to exclude contamination by genomic DNA. Upon treatment, DNase was heat denatured for 10 minutes at 65°C. To further exclude genomic amplifications, PCR was performed with specific DNA primers for RLN2 and RXFP2 as well as 18S rRNA, which all spanned at least one intron. We did not observe PCR amplification using total RNA as a template. Five hundred nanograms of total RNA was used for each cDNA reaction. The cDNA was generated with 50 ng/μL (20 pmol) oligo-dT_{15} primer (Amersham Pharmacia Biotech, Uppsala, Sweden) and 0.8 μL Superscript RNase H^- reverse transcriptase (100 U; Life Technologies, Paisley, UK) for 60 minutes at 37°C.

Reverse Transcriptase–Polymerase Chain Reaction (RT-PCR)

RT-PCR amplifications were carried out with 2 μL cDNA in a final volume of 20 μL containing 0.15 μL Taq polymerase, 1 μL 50 mM $MgCl_2$, 2 μL PCR buffer, 0.5 μL dNTP, and 0.5 μL forward/reverse primer mix (synthesized at MWG Biotech AG, Ebersberg, Germany), using the following primer combinations: RLN2, forward, 5′-tctgtttac tactgaaccaattt-3′ and reverse, 5′-catggcaacatttattagccaa-3′; RXFP1, forward, 5′-tctgcccattaacagtgctttg-3′ and reverse, 5′-gtatgt gaaaaggtccggcttc-3′; RXFP2, forward, 5′-tgcacagagagcacagcagaatggctc-3′ and reverse, 5′-ggacagtgcaacccgatgtgaaagacc-3′; 18S rRNA, forward, 5′-actcaacacgggaaacctcacc-3′ and reverse, 5′-cgctccaccaactaagaacgg-3′. After 3 minutes of heat denaturation at 94°C, the PCR cycle consisted of (1) 94°C for 30 seconds; (2) 55°C (RLN2), 60°C (RXFP1), 65°C (RXFP2), 55°C (18S) for 45 seconds each; and (3) 72°C for 1 minute. For each primer pair, 40 cycles were performed, and a final elongation step of 72°C for 7 minutes completed the PCR run. Ten microliters of the PCR reaction was loaded onto a 1% agarose gel, and the expected amplicons were visualized via fluorescence (RLN2 transcript variant 1: 487 bp; RLN2 transcript variant 2: 587 bp; RXFP1: 214 bp; RXFP2: 240 bp; 18S rRNA: 111 bp). Base pair values were compared with gene bank data, and PCR products were confirmed by BigDye sequencing (Applied Biosystems, Foster City, CA).

Real-Time RT-PCR for MMP2, MMP9, MMP13, TIMP1, and TIMP2

Samples were analyzed by real-time RT-PCR using an Opticon 2 system (MJ Research, Waltham, MA). Reactions were performed using SYBR green master mix (Applied Biosystems, Darmstadt, Germany) as a double-stranded DNA-specific fluorescent dye, with the appropriate primer sets (Table 1). 18S rRNA was used because its expression was not influenced by any of the mediators investigated. PCR was initiated with 2 minutes at 50°C, followed by 1.5 minutes at 95°C. The program continued with 30 cycles of 20 seconds at 95°C and 60 seconds at 60°C. Each assay included duplicates of each cDNA sample and a nontemplate negative control for MMP2, MMP9, MMP13, TIMP1, and TIMP2. The cycle threshold (CT) parameter is defined as the cycle number at which fluorescence intensity exceeds a fixed threshold. Relative amounts of mRNA expression were calculated using the ΔΔCT method.[24] The expression of 18S rRNA was used to normalize samples for the amount of cDNA used per reaction. To confirm the amplification, the resulting real-time PCR products were analyzed by dissociation curves, and amplicons were confirmed by BigDye termination sequencing.

RLN2 ELISA

Tears were collected from healthy volunteers (female: $n = 31$; male: $n = 17$) without autoimmune diseases due to possibility of assay interference. RLN2 released in tears and RLN2 concentrations in

Downloaded from iovs.arvojournals.org on 06/17/2019

Table 1. Primer Used for Real-Time RT-PCR

Name	Primer (5′–3′)	Size, bp
MMP2	Forward, ggcctctcctgacattgacctt Reverse, ggcctcgtataccgcatcaatc	241
MMP9	Forward, gggcttagatcattcctcagtg Reverse, gccattcacgtcgtccttat	94
MMP13	Forward, agaccccaaccctaaacatccaaaaac Reverse, ttaaaaacagctccgcatcaacct	155
TIMP1	Forward, acttccacaggtcccacaac Reverse, agccacgaaactgcaggtag	96
TIMP2	Forward, gagcctgaaccacaggtacca Reverse, aggagatgtagcacgggatca	77
18S rRNA	Forward, actcaacacgggaaacctcacc Reverse, cgctccaccaactaagaacgg	111

samples from human cadaveric cornea ($n = 2$), eyelid ($n = 4$), lacrimal gland ($n = 6$), nasolacrimal ducts ($n = 1$), and prostate ($n = 1$), as well as three samples of amniotic membranes, were measured with an enzyme-linked immunosorbent assay (ELISA), purchased from Immundiagnostik (Bensheim, Germany). The assay kit contained all antibodies and other necessary components, and the assay was performed according to the manufacturer's instructions. Schirmer strips (Gecis, Lamotte-Beuvron, France) used to collect the tears were stored at −20°C until processed. Strips from both eyes were pooled, 50 μL sample dilution buffer (Immundiagnostik) was added, and centrifugation was performed to extract the tears. Tissue samples were crushed in an agate mortar under liquid nitrogen, then homogenized in 300 μL 1% Triton buffer (Triton X-100; Carl Roth, Karlsruhe, Germany) with a protease and phosphatase inhibitor cocktail (Fermentas, St. Leon-Roth, Germany). The samples were centrifuged at 13,000 rpm for 30 minutes. Total protein content was measured with a protein assay (Bio-Rad, Munich, Germany). Human recombinant (r) RLN2 at the concentrations of 0, 3.1, 9.3, 28, 83, and 250 pg/mL served as the standard. The detection limit of this assay was 3.1 pg/mL. Concentrations were calculated in relation to total protein concentration. The assay was validated for the use of tears by spiking of tear samples with known concentrations of recombinant RLN2.

Cell Proliferation Assay

A colorimetric BrdU (5-bromo-2′-deoxyuridine) cell proliferation ELISA (Roche Diagnostics, Mannheim, Germany) was used according to the manufacturer's instructions. Briefly, 80% confluent, growing cells were stimulated for 24 hours with 100 ng/mL or 500 ng/mL rRLN2 and were incubated at 37°C in a water-saturated CO_2 incubator. After 18-hour stimulation, 10 μM BrdU labeling solution was added to each well of a 96-well plate, except for negative controls that received no BrdU, and remained for 6 hours. Then, plates were drained and blocked with 200 μL/well of precooled ELISA fixative for 30 minutes at −20°C. After decanting, 100 μL anti-BrdU-POD (peroxidase) was added to each well, and dishes were incubated for 30 minutes at 37°C. Plates were drained, washed, and incubated with 100 μL/well anti-BrdU working solution for 30 minutes at 37°C. Finally, 100 μL peroxidase substrate was added to each well and incubated for 1 minute on a shaker at 300 rpm; absorbance was measured within 5 minutes at 405 nm in an ELISA reader (SLT LAB Instruments, Crailsheim, Germany).

Migration Assay

In vitro wound modeling was performed using a scratch assay. Confluent monolayers of HCE and HCjE on glass coverslips in six-well plates were scratched with a 200 μL plastic pipette tip to create a cell-free area. Cultures were gently washed three times with DMEM to remove loose cells. DMEM was added plus or minus 100 ng/mL rRLN2, and cells were incubated for 24 hours in a CO_2 incubator. In addition, cultures treated with 100 ng/mL rRLN2 were also treated for 24 hours with 5 μg/mL mitomycin C (purity ≥97%; Sigma-Aldrich) or with 5 μM cytochalasin B (purity ≥98%; Sigma-Aldrich). Mitomycin C was dissolved in dimethylsulfoxide (DMSO). After washing, cells were fixed for 5 minutes in 4% paraformaldehyde. Repeated washing was followed by staining of the cells with hematoxylin/eosin (HE). Glass coverslips were examined with an Axiophot microscope (Zeiss, Jena, Germany). Nine fields of each scratch area were photographed, and the cell-free width was determined. For comparison, three slides were stained at time zero and photographed. The average width of the scratch closure area was calculated.

Corneal Wound In Vivo Experiments

To produce corneal wounds, mice were anesthetized by an intraperitoneal injection of ketamine (90 mg/kg body weight, Ketavet 100 mg/mL; Pharmacia, Berlin, Germany) and xylazine (6 mg/kg body weight, Rompun 2%; Bayer, Leverkusen, Germany). Conjucain EDO eye drops (Bausch & Lomb, Berlin, Germany) were applied to the cornea as a topical anesthetic for pain relief postoperatively. Corneal wounds were produced as previous described.[25] In brief, on the right eye of each animal, an alkali-soaked (0.5 M NaOH) filter paper disk (Whatman filter paper, grade 41, 20–25 μm; Whatman, Dassel, Germany) 2 mm in diameter was placed on the central surface of the cornea for 2 minutes followed by rinsing in 0.9% sterile saline (Fresenius Kabi, Bad Homburg, Germany). The left eye of each mouse was left untreated and served as a control for normal cornea. After producing a defined central corneal ulcer 2 mm in diameter, the corneas were allowed to partially heal in vivo for up to 6 hours. At the end of this period, mice were sacrificed, and the eyes were enucleated with an anatomical forceps (Geuder, Heidelberg, Germany). Each eye was transferred to a well whose bottom contained a 3 mm thick dental wax layer and was pinned to the wax with a sterile needle (27G × 3/4 inch Sterican; B. Braun, Melsungen, Germany), adjusting the corneal surface to face upward. Each well received 1 mL DMEM medium supplemented with amphotericin B (2.5 μg/mL; Biochrom AG), 50 IU/mL penicillin, and 50 μg/mL streptomycin to cover the eyes completely. The eyes were randomly assigned to a control group, a 30 ng/mL rRLN2 group, and a 100 ng/mL rRLN2 group. Corneal wounds in the control group (10 eyes) received 1 mL medium. Treatment groups received 30 ng/mL or 100 ng/mL RLN2 in medium at 0, 6, 12, 18, 24, 30, 36, 42, 48, 54, 60, 66, 72, and 84 hours after alkali-induced corneal wounding, respectively. The eyes were maintained in a tissue culture incubator (Heraeus, Hanau, Germany) at 37°C (5% CO_2 and 21% O_2). To monitor the corneal healing process, images were taken by a Micron III unit (Phoenix Research Laboratories, Pleasanton, CA) generating a blue light. The corneal wounds were visualized by applying sodium fluorescein eye drops (Fluoreszein SE Thilo; Alcon, Fort Worth, TX). The imaged area of corneal defects was evaluated using the SigmaScan Pro 5.0 software (Systat Software Inc., San Jose, CA).

Downloaded from iovs.arvojournals.org on 06/17/2019

Table 2. Percentage of Positive Tissues for RLN2, RXFP1, and RXFP2 Detected by RT-PCR

	Lacrimal Gland	Eyelid	Conjunctiva	Cornea	Primary Corneal Fibroblasts	Nasolacrimal Ducts
RLN2	9	60	14	29	0	25
RXFP1	20	60	67	40	100	75
RXFP2	73	100	50	64	100	75

Positive tested tissues (%), $n \geq 4$ for each tissue.

Statistical Analysis

Data are expressed as mean ± SEM. After evaluating values on normal distribution using Kolmogorov–Smirnov test (all variables were normally distributed), we performed one-way ANOVA statistics. For the interpretation of the results we used either Bonferroni or Games-Howell post hoc test depending on Levene's test for homogeneity of variances. To compare the corneal epithelial healing after alkali-induced wounds between the control, 30 ng/mL rRLN2, and 100 ng/mL rRLN2 groups, the wound areas were measured at different time points, and Kaplan-Meier analysis was performed. The terminal event was defined as complete healing of the corneal wounds. Statistical significance among groups was analyzed by the log-rank test. A P value less than 0.05 was considered statistically significant. All data were analyzed by IBM SPSS Statistics software package version 19.0 (IBM SPSS, Chicago, IL). A P value less than 0.05 was considered statistically significant.

Results

RLN2 Expression in Tissues of the Ocular Surface, in the Lacrimal Apparatus, and in Human Tears

Specific amplicons encoding RLN2 transcript variant 2 (587 bp) were detected in lacrimal gland, conjunctiva, cornea, nasolacrimal duct, and eyelids (Table 2; Fig. 1). RLN2 transcript variant 1 (487 bp) was detected in lacrimal gland, eyelids, and nasolacrimal ducts, but not in conjunctiva and cornea. Primary corneal fibroblasts were devoid of both RLN2 transcript variants. 18S rRNA served as internal control for each sample. An RLN2-specific ELISA was performed to quantify and determine RLN2 concentration in vivo in different tissues of the ocular surface and in the tear fluid of healthy volunteers.

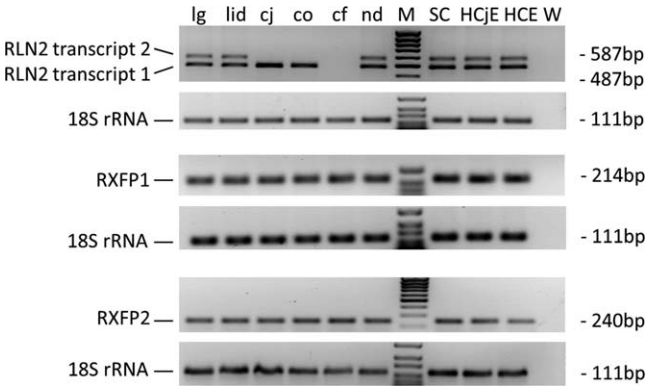

Figure 1. Ethidium bromide–stained agarose gel for visualization of RT-PCR amplification products derived from the following tissues ($n \geq 4$ for each tissue): lacrimal gland (lg), eyelid (lid), conjunctiva (cj), cornea (co), primary corneal fibroblasts (cf), and nasolacrimal ducts (nd). PCR amplification products derived from human sebaceous (SC), conjunctival (HCjE), and corneal (HCE) cell lines. DNA marker (M); water control (W) indicates the negative control without template cDNA.18S rRNA served as a PCR control for equal cDNA loading.

RLN2 protein was detectable in lacrimal gland, eyelids, cornea, nasolacrimal duct, amniotic membrane, and prostate (Table 3), with highest concentration measured in the lacrimal gland (up to 33.04 pg/mg). RLN2 in tears was below the detection limit in 18 out of 48 tear samples (Table 4). The detectable concentrations in the tears obtained from healthy male volunteers varied from 0.12 to 36.8 pg/mg total protein. By contrast, tears collected from pregnant (first trimester) and nonpregnant female volunteers contained only very low concentrations RLN2 protein (0.4–0.64 pg RLN2/total protein [mg]).

RXFP1 and RXFP2 Transcripts Are Expressed in Tissues of the Lacrimal Apparatus and Ocular Surface

Specific RXFP1 and RXFP2 amplicons at the expected 214 bp and 240 bp, respectively, were detected in lacrimal gland, eyelid, conjunctiva, cornea, nasolacrimal ducts, and primary corneal fibroblasts (Table 2; Fig. 1). In all tissues investigated, 18S rRNA confirmed the presence of similar amounts of cDNA for RT-PCR.

RLN2, RXFP1, and RXFP2 Are Present in Cell Lines of Ocular Origin

Specific amplicons for RLN2 transcript variant 1 (487 bp) and RLN2 transcript variant 2 (587 bp) were observed in SC, HCjE, and HCE cells (Fig. 1). SC, HCjE, and HCE cells presented RXFP1 and RXFP2 amplification products at 214 bp, and 240 bp, respectively. SC served as an in vitro model for meibomian glands. Isolated protein RLN2 from HCjE and HCE cells was detectable by ELISA (Table 5). Secreted RLN2 in supernatant from SC, HCjE, and HCE reached highest concentrations in SC (217.99 pg/mg) and lowest in HCE (0.79 pg/mg).

rRLN2 Promotes Proliferation of SC, HCjE, and HCE

A slight increase in proliferation of SC cells, by 1.3-fold, was detected upon 24-hour stimulation with 500 ng/mL RLN2 (Fig. 2), whereas 100 ng/mL rRLN2 had no effect. A somewhat higher proliferative response was detected in HCjE cells, which showed a 1.9- and 1.7-fold increase in DNA synthesis at 100 ng/mL and 500 ng/mL rRLN2, respectively. Regardless of the concentration of rRLN2 used, HCE cells showed a 1.3-fold increase in DNA synthesis. Proliferation of primary corneal fibroblasts was not influenced by rRLN2 (data not shown).

rRLN2 Promotes Migration of HCjE and HCE

HCjE cells stimulated with 100 ng/mL rRLN2 for 24 hours showed no significantly higher scratch closure rate as compared to untreated cells (Fig. 3). rRLN2 (100 ng/mL) stimulation induced migration of HCjE cells at a rate similar to the closure rate of cells treated with 30 ng/mL rhEGF. Both treatment with the motility inhibitor cytochalasin B and

Downloaded from iovs.arvojournals.org on 06/17/2019

Table 3. ELISA Analysis of RLN2 Protein in Human Tissue

	Lacrimal Gland	Lid	Cornea	Nasolacrimal Duct	Amniotic Membrane	Prostate
Detectable samples, *n*	6/6	4/4	2/2	1/1	3/3	1/1
Mean (range)	8.04 (0.91–33.04)	4.16 (1.10–8.79)	1.97 (1.04–2.90)	0.85	2.02 (1.45–2.68)	3.64

RLN2 concentrations are expressed as mean (RLN2 protein [pg]/total protein [mg]).

treatment with the proliferation inhibitor mitomycin C had little effect on the scratch closure rate.

HCE cells stimulated with 100 ng/mL rRLN2 for 24 hours showed a significantly higher scratch closure rate as compared with unstimulated cells (Fig. 3). To determine whether this effect could be ascribed to increased proliferation and/or migration, treatment with cytochalasin B, an inhibitor of migration, was used. In the presence of cytochalasin B, negligible cellular movement over the scratch area was observed. In contrast, treatment of the cells with mitomycin C resulted in the inhibition of proliferation, so the observed scratch closure can be ascribed to migration. Thus, the main effect of RLN2 in scratch closure pertained to increased cell migration. Recombinant hEGF induced strong promigratory action, comparable to the closure rate of HCE cells treated with 100 ng/mL RLN2. The addition of an equivalent concentration of the mitomycin C solvent DMSO for 24 hours alone resulted in a negligible change in migration (data not shown).

RLN2 Regulates MMP2, MMP9, TIMP1, and TIMP2 in SC, HCjE, and HCE

SC, HCjE, and HCE cell lines were incubated with rRLN2 at different concentrations for 6 and 24 hours prior to real-time PCR detection of transcript levels for MMP2, MMP9, MMP13, TIMP1, and TIMP2.

Real-time RT-PCR revealed induction of MMP2 mRNA in SC upon 24-hour stimulation with 100 ng/mL RLN2 (Fig. 4A). Shorter exposure time (6 hours) or higher concentrations of rRLN2 (500 ng/mL) added had no significant effect on mean MMP2 mRNA concentrations. Basal MMP9 mRNA levels increased 3.3-fold at 6 hours of exposure to rRLN2 at both 100 ng/mL and 500 ng/mL (Fig. 4B). No significant change was observed at 24-hour treatment with rRLN2. MMP13 mRNA levels were not significantly influenced by rRLN2 (data not shown). Basal TIMP1 transcript levels were upregulated in SC exposed to rRLN2 (100 ng/mL) for 24 hours (Fig. 4C). At 6-hour stimulation with 500 ng/mL rRLN2, TIMP1 mRNA levels increased 2.7-fold. Neither the exposure for 6 hours with 100 ng/mL RLN2 nor for 24 hours with 500 ng/mL influenced TIMP1 levels significantly. Furthermore, TIMP2 transcription was not affected by RLN2 in SC.

In HCjE, real-time PCR revealed a significant induction of MMP2 mRNA, by 1.8-fold, upon 24-hour stimulation with 100 and 500 ng/mL rRLN2 as well as 6-hour stimulation with rRLN2 at 500 ng/mL (Fig. 5A). By contrast, 100 ng/mL rRLN2 for 6 hours had no effect. MMP9 expression was significantly affected by 100 ng/mL rRLN2 at 6 hours (Fig. 5B). MMP13 was augmented 1.8-fold in HCjE only after 6-hour incubation with 500 ng/mL rRLN2 (not shown). TIMP1 mRNA levels were downregulated to 60% after 6-hour incubation with 100 ng/mL RLN2. At higher concentration of rRLN2 (500 ng/mL), we observed a significant 2.0-fold increase of TIMP1 expression in HCjE (Fig. 5C). Upregulation of TIMP2 after 24 hours was detected upon stimulation with 100 ng/mL rRLN2. Incubation with rRLN2 at 500 ng/mL for 6 hours also induced a significant 2.0-fold augmentation of TIMP2 mRNA expression (Fig. 5D).

In HCE, real-time RT-PCR revealed induction of MMP2 mRNA by up to 1.8-fold upon 24-hour stimulation with rRLN2, both at 100 ng/mL and at 500 ng/mL. A 6-hour treatment had no significant effect (Fig. 6A). MMP9 (Fig. 6B) and MMP13 mRNA levels (data not shown) were unaffected after rRLN2 treatment. TIMP1 expression was upregulated 2.0-fold with treatment for 24 hours with rRLN2 (Fig. 6C). Exposure to 100 ng/mL rRLN2 for 6 hours elevated both TIMP1 and TIMP2 mRNA concentrations (Figs. 6C, 6D). Apart from this change in TIMP2 expression, no other concentration of rRLN2 was effective in changing TIMP2 mRNA levels in HCE.

rRLN2 Promotes Re-epithelialization of Corneal Ulcers

To study potential therapeutic effects of exogenously administered rRLN2 on corneal wound healing and repair, we utilized a combined in vivo/in vitro corneal defect model in mice.[25] In this model, corneal lesions were allowed to partially heal in vivo for 6 hours followed by enucleation of the eyeball and cultivation in vitro in medium. After dividing 30 eyes randomly into the control and treatment groups, medium was carefully applied onto the surface of the corneal wounds in the control group, whereas the treatment group received medium supplemented with 30 and 100 ng/mL rRLN2 on the corneal wound area in the same way. The healing process was documented every 6 hours by visualization of the remaining corneal wound area with fluorescein solution, and the medium was replaced for each image. Kaplan-Meier wound healing curves with the log-rank test revealed a statistically significant difference between control and the 100 ng/mL rRLN2 group ($P = 0.002$) and between control and 30 ng/mL rRLN2 and 100 ng/mL rRLN2 ($P = 0.023$) (Fig. 7). Control eyes showed a healing tendency, but no defect healed completely within 86 hours (Fig. 7B). When treated with 30 ng/mL RLN2, 40% of the eyes healed completely. Only when treated with 100 ng/mL

Table 4. ELISA Analysis of RLN2 Protein in Human Tears

		Female	
	Male	Nonpregnant	Pregnant
Detectable samples, *n*	9/17	4/24	5/7
Mean (range)	4.34 (0.12–36.80)	0.64 (0.18–1.50)	0.40 (0.13–0.99)

RLN2 concentrations are expressed as mean (RLN2 protein [pg]/total protein [mg]).

Table 5. ELISA Analysis of RLN2 Protein in Cell Lines

	SC	HCjE	HCE
Protein	–	10.52	2.72
Supernatant	217.99	21.55	0.79

RLN2 concentrations are expressed as mean (RLN2 protein [pg]/total protein [mg]).

Downloaded from iovs.arvojournals.org on 06/17/2019

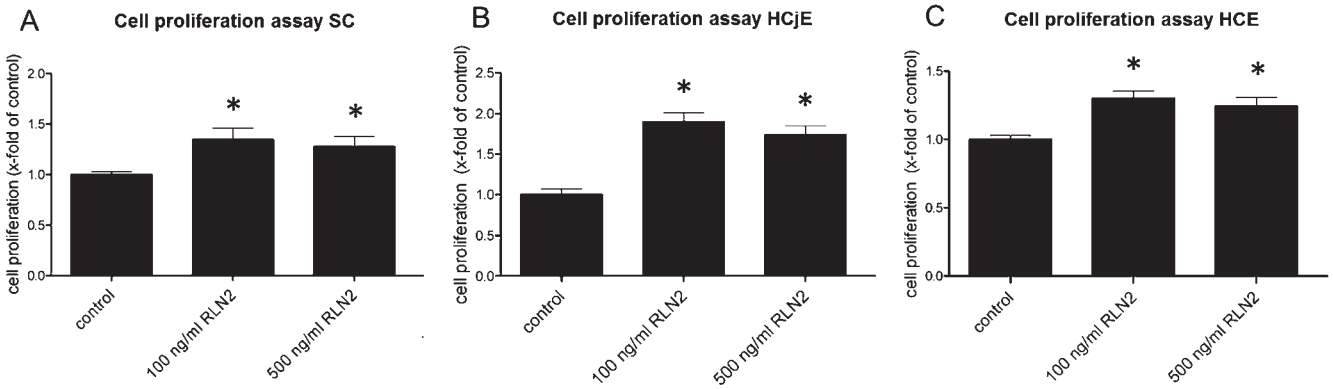

Figure 2. Nonradioactive BrdU proliferation assays on human sebaceous (SC) (**A**), conjunctival (HCjE) (**B**), and corneal (HCE) (**C**) cell lines exposed to 100 ng/mL and 500 ng/mL RLN2 for 24 hours. Results of the proliferation assays are shown as mean ± SEM ($n = 9$; $^*P < 0.05$).

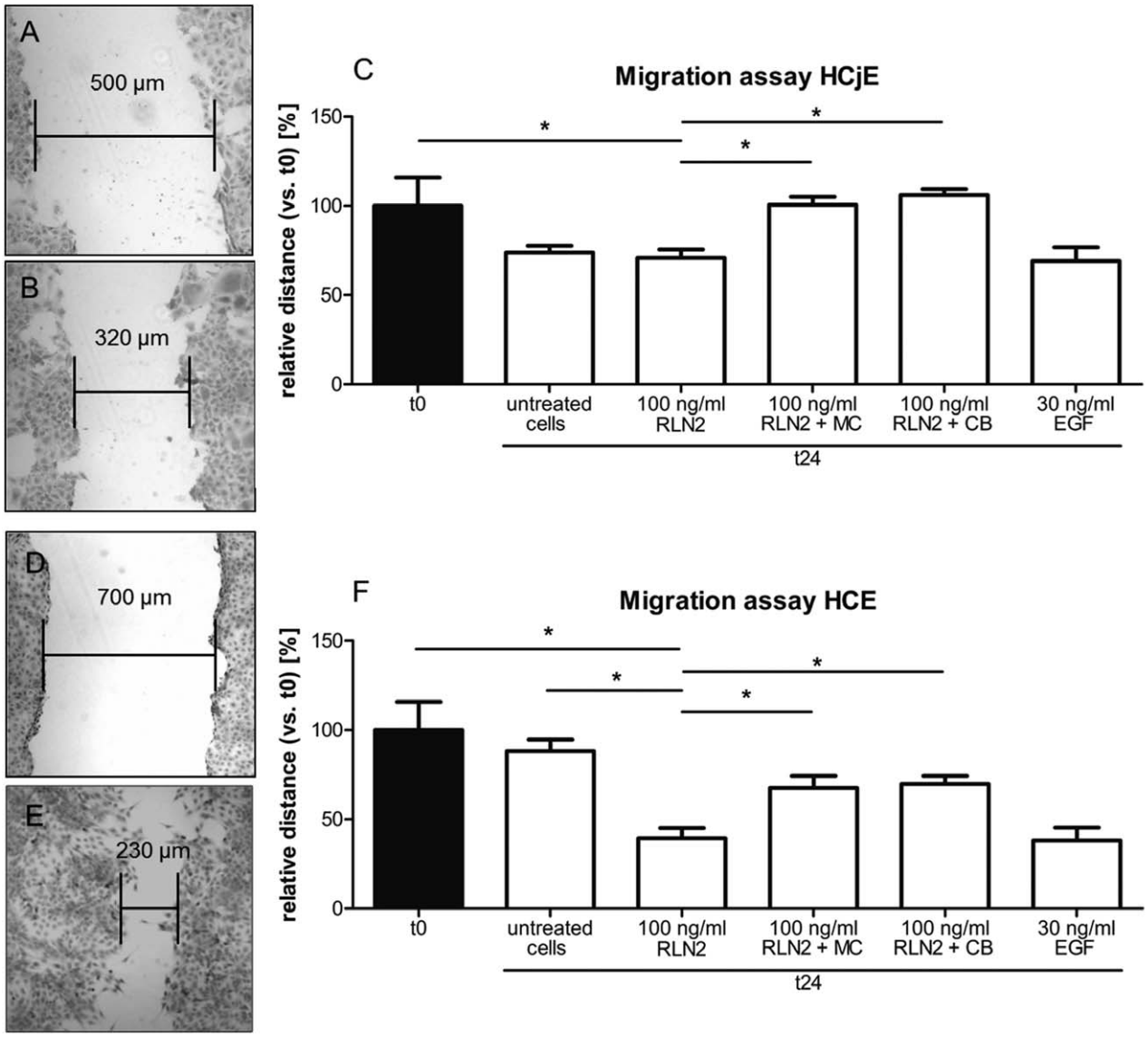

Figure 3. Scratch assay and the effect of 100 ng/mL RLN2 on the migration of human conjunctival epithelial cell line (HCjE) (**A–D**) and human corneal epithelial cell line (HCE) (**E–H**). Enhanced migration of cells into the scratch wound resulted in shorter distances measured between the two opposing cell borders of a scratch. (**A**, **D**) Control, 0 hours; cells were just removed and washed. (**B**, **E**) Cells stimulated with 100 ng/mL RLN2 for 24 hours. (**C**, **F**) Cell migration assays represented by relative distance ± SEM. The relative distances after 24 hours relate to the initial scratch distance (t0). ($n = 18$, $^*P < 0.05$). MC, mitomycin C; CB, cytochalasin B; EGF, epithelial growth factor.

Downloaded from iovs.arvojournals.org on 06/17/2019

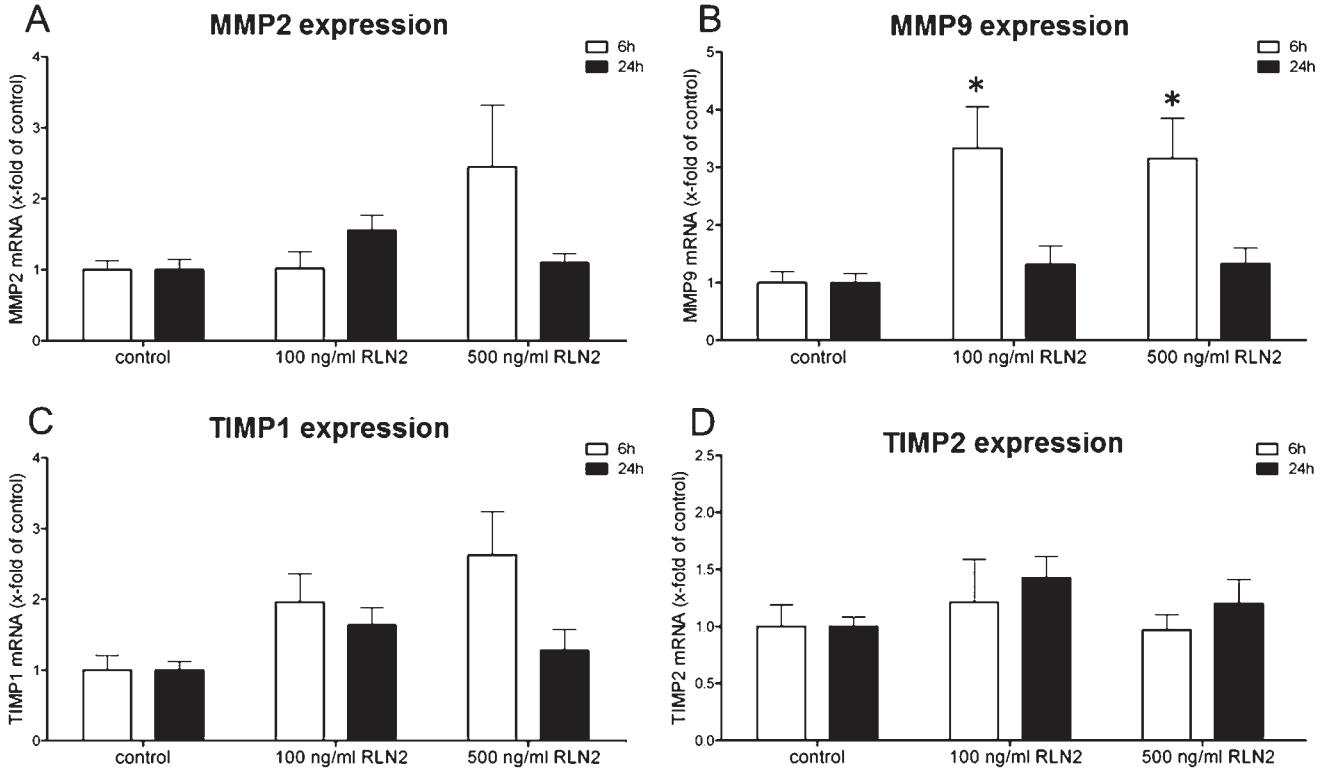

Figure 4. Real-time RT-PCR of human sebaceous cell line (SC). Cells were stimulated for 6 hours (*white bar*) or 24 hours (*dark bar*) with 100 ng/mL and 500 ng/mL RLN2. The fold increase in MMP2 (**A**), MMP9 (**B**), TIMP1 (**C**), and TIMP2 (**D**) transcript levels was expressed as mean ± SEM; statistical significance ($n = 9$; $^*P < 0.05$) is indicated by the *asterisk*.

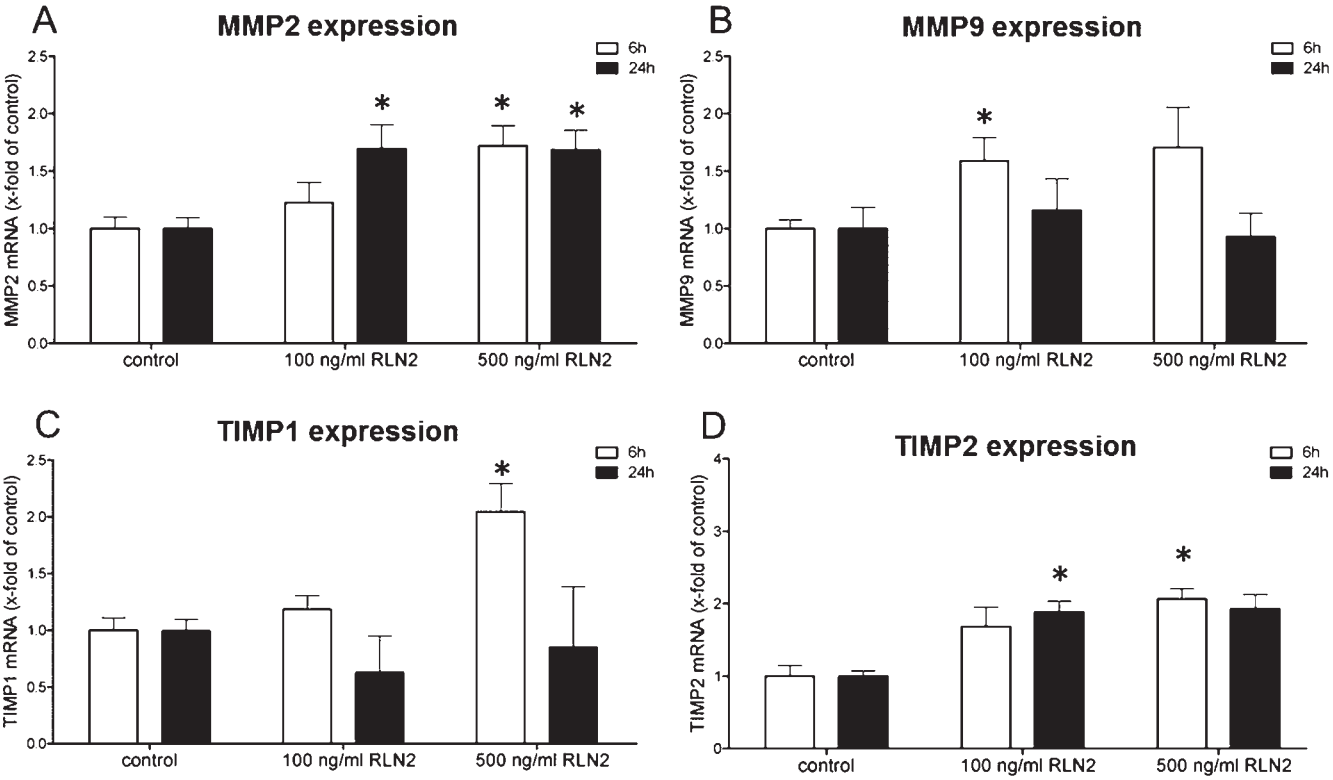

Figure 5. Real-time RT-PCR on human conjunctival epithelial cell line (HCjE). Cells were stimulated for 6 hours (*white bar*) or 24 hours (*dark bar*) with 100 ng/mL and 500 ng/mL RLN2. The fold increase in MMP2 (**A**), MMP9 (**B**), TIMP1 (**C**), and TIMP2 (**D**) transcript levels was expressed as mean ± SEM; statistical significance ($n = 9$; $^*P < 0.05$) is indicated by the *asterisk*.

Downloaded from iovs.arvojournals.org on 06/17/2019

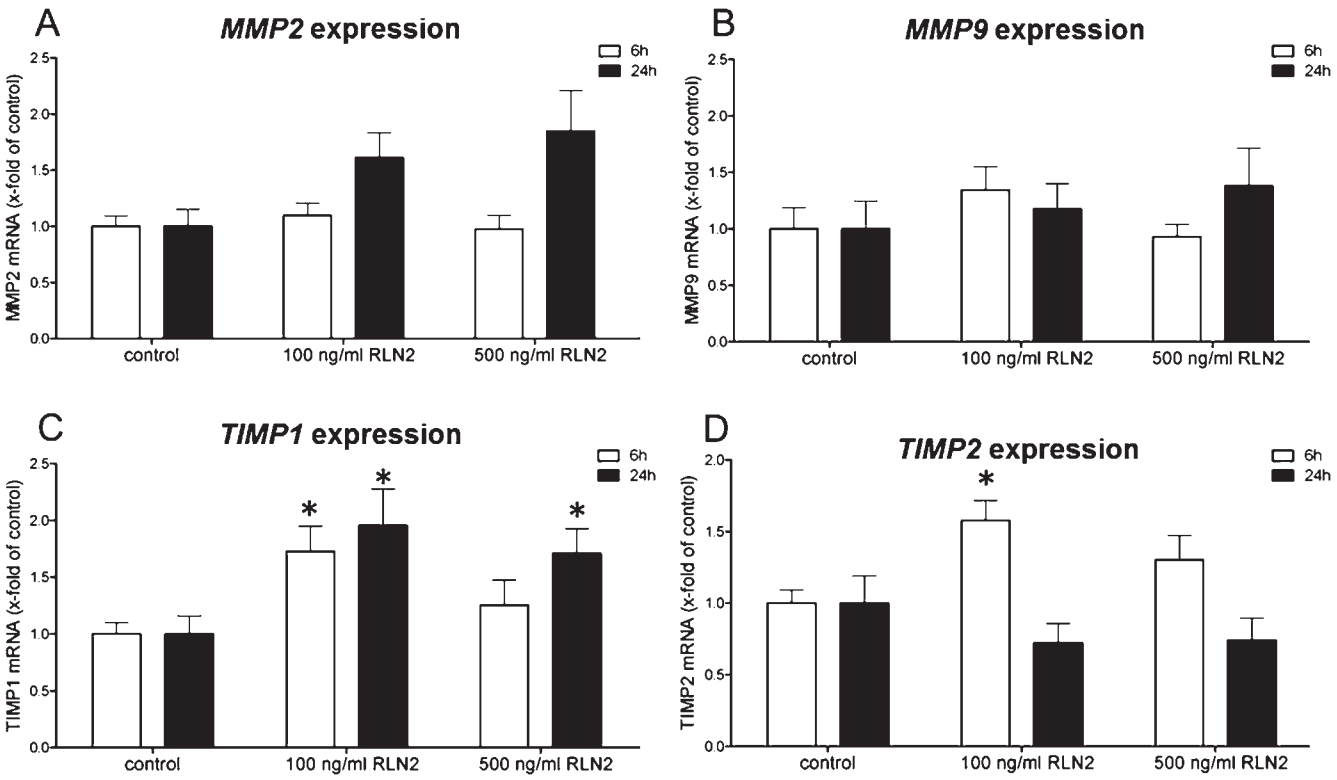

Figure 6. Real-time RT-PCR of human corneal cell line (HCE). Cells were stimulated for 6 hours (*white bar*) or 24 hours (*dark bar*) with 100 ng/mL and 500 ng/mL RLN2. The fold increase in MMP2 (**A**), MMP9 (**B**), TIMP1 (**C**), and TIMP2 (**D**) transcript levels was expressed as mean ± SEM; statistical significance ($n = 9$; $^*P < 0.05$) is indicated by the *asterisk*.

rRLN2, all corneal wounds were closed after 54-hour treatment. With these data taken together, topical application of rRLN2 on corneal ulcers produced by alkali injury significantly accelerated the re-epithelialization of the corneal wounds.

Discussion

This is the first report on the hormone RLN2 and its cognate receptors, RXFP1 and RXFP2, at the ocular surface and in the lacrimal apparatus. The detection of transcripts for RXFP1 and RXFP2 in the lacrimal gland, eyelids, conjunctiva, cornea, nasolacrimal ducts, and primary corneal fibroblasts identifies the ocular surface and the lacrimal apparatus as a novel physiological target of the actions of RLN2.

Both RLN2 transcript variants 1 and 2 were detected in lacrimal glands, eyelids, and nasolacrimal ducts, whereas RLN2 transcript variant 1 was exclusively detected in cornea and conjunctiva. Both RLN2 transcript variants have been reported in human placenta and prostate gland.[26] The larger RLN2 amplicon contains an additional 101 bp exon in the C peptide region that is incorporated through alternative splicing. This creates a stop codon within the C peptide region, and the deduced (pro)RLN2 peptide consists of the B-chain with deficient A-chain, likely rendering this product biologically nonfunctional. The physiological relevance of this larger mRNA product is currently unknown, in part due to the lack of suitable antibodies capable of detecting this truncated RLN2 form. The human ocular tissues were obtained from cadaveric specimens, and we cannot exclude that RNA degradation may have contributed to reduced or lacking mRNA levels observed in some of these tissues. Nevertheless, we detected immunoreactive RLN2 protein by ELISA in lacrimal gland, lid, cornea, and nasolacrimal duct, as well as in amniotic membrane and prostate used as positive control. Thus, we identified human ocular tissues as a novel source of RLN2. Next, we wondered if RLN2 was present in tear fluid. It is conceivable that RLN2 is transported via the bloodstream and secreted into the tear fluid, thus acting as a paracrine hormone at the ocular surface. RLN2 is structurally related to insulin, which has been shown to be secreted into the tear fluid.[27] Further, RLN2 has been measured in serum and other body fluids,[28] including urine, where relaxin serves as pregnancy marker in certain species.[29–31] Here, we showed that low levels of RLN2 were detectable in human tears. As Schirmer strips (Gecis) were used for tear collection, it has to be considered that measured RLN2 levels represent a combination of serum proteins and proteins of conjunctival origin. We found no difference in RLN2 levels present in tear fluids collected from males or females, nor did we observe a significant difference in RLN2 levels in tears between first-trimester pregnant women and nonpregnant women. These data suggest that RLN2 levels in tears seem not to correspond with serum levels, as RLN2 serum concentrations are elevated during the first trimester in pregnancy.[32]

We employed the human sebaceous (SC), conjunctival epithelial (HCjE) and corneal epithelial (HCE) cell lines to study the potential functions of relaxin and its cognate receptors RXFP1 and RXFP2 at the ocular surface and the lacrimal apparatus. SC served as an in vitro model for meibomian glands, which are large specialized sebaceous glands in the eyelids that deliver the majority of the lipid layer of the tear film.[23] Skin sebaceous glands and meibomian glands are holocrine glands, and both are influenced by hormones. However, our findings are limited, as the results for skin sebaceous cells might differ from those for meibomian cells. All three cell lines expressed RLN2 (transcript variant 1 and 2) as well as RXFP1 and RXFP2 transcripts and were responsive to

Downloaded from iovs.arvojournals.org on 06/17/2019

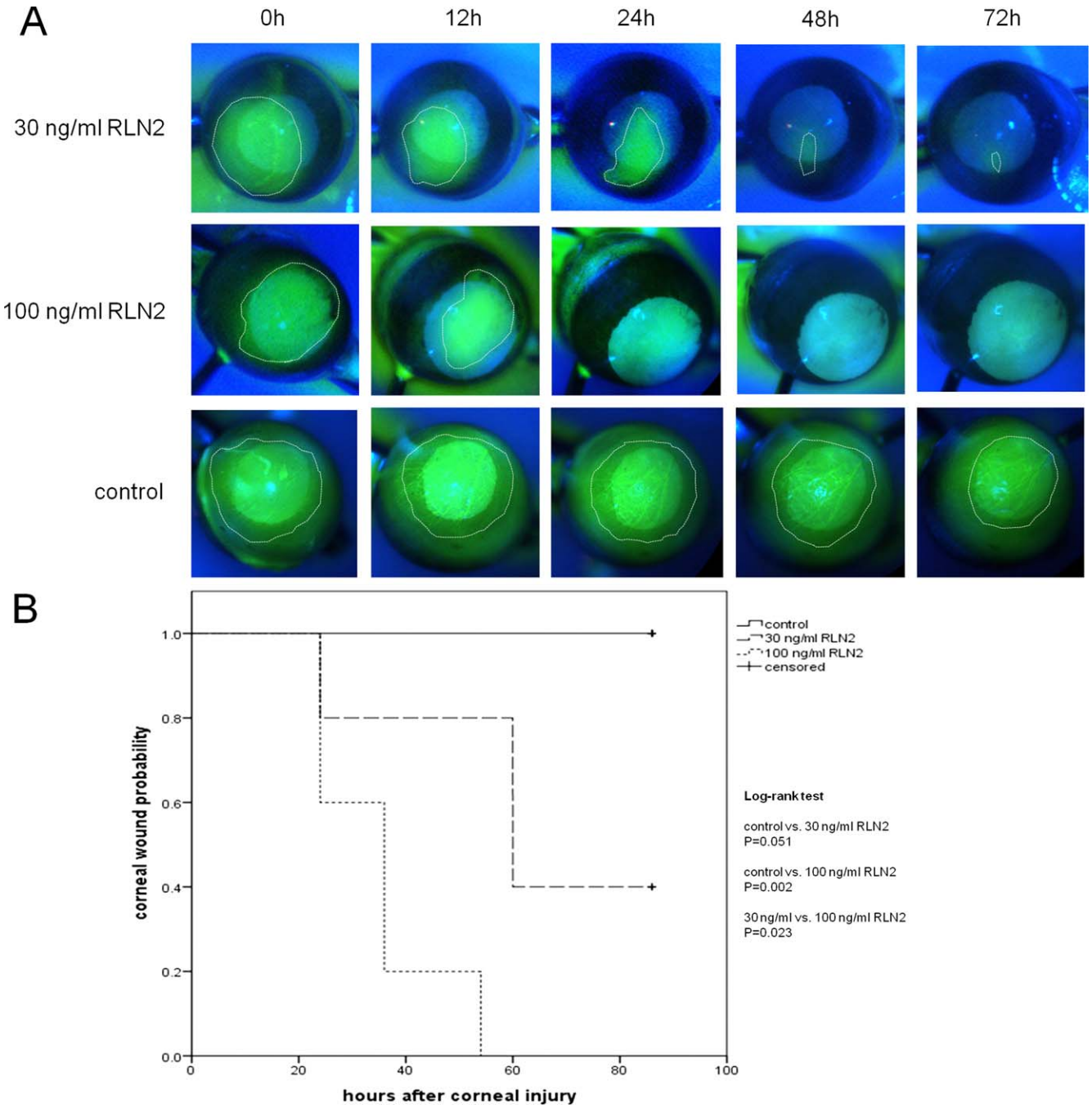

FIGURE 7. Corneal re-epithelialization upon alkali wounding and treatment with 30 ng/mL or 100 ng/mL RLN2. (**A**) Photographs show representative fluorescein-stained corneal wounds of the control, 30 ng/mL RLN2, and 100 ng/mL RLN2 groups at different time points during healing process. The edges of the wound areas are marked with *white dotted lines*. Wound areas were quantified using the software SigmaScan Pro 5.0. (**B**) Kaplan-Meier curves show the probability of corneal wound healing at different time points in control, 30 ng/mL RLN2, and 100 ng/mL RLN2 groups. Censored cases are indicated by small vertical *tick marks*. Corneal re-epithelialization was significantly enhanced by local application of RLN2 onto the wounded corneal surface.

rRLN2, suggesting that RLN2 at pharmacological doses may be useful in promoting ocular wound healing.[33–36]

The role of RLN2 in proliferation appears to be cell type specific. Relaxin has been shown to cause a significant dose-related increase in human amniotic epithelial cell proliferation over 5 days.[37] In contrast, reports from various cancer cell models failed to demonstrate a strong mitogenic effect of relaxin.[33,38,39] Similarly, analyses on cardiac fibroblasts could not find any marked effect of rRLN2 on proliferation.[34] In our ocular cell models, rRLN2 induced a modest proliferative response in SC, HCjE, and HCE cells when stimulated for 24 hours. This may reflect a cell type–specific regenerative function of RLN2 at the ocular surface and the lacrimal apparatus to ensure the repair of frequently occurring ocular surface injuries.

The migration of ocular cells into sites of ocular surface injury is a major component of the corneal/conjunctival wound healing response. Intriguingly, rRLN2 markedly increased the migration of HCE cells, which under physiological

Downloaded from iovs.arvojournals.org on 06/17/2019

conditions serve to restore an intact ocular surface.[1] While factors other than RLN2 seem to act as more potent stimulators of proliferation in HCjE and HCE cells, RLN2 may serve an important role in promoting the increased migration of corneal cells into denuded ocular surfaces. A similar concept has been shown using monolayers of bronchial epithelial cells in a wound-healing model in which relaxin augmented wound closure.[40] In different cancer cell models, RLN2 has been shown to increase tumor cell motility.[33,38,41] Our results support the hypothesis that the promigratory activity induced by rRLN2 enhances corneal epithelial repair and identify a new role of RLN2 as a protective hormone at the ocular surface.

Some of the effects of RLN2 are based on its ability to induce the expression and enhance the catalytic activity of matrix metalloproteinases (MMPs). MMPs and their physiological antagonists, the tissue inhibitors of matrix metalloproteinases (TIMPs), play an important role in wound healing and tissue remodeling. RLN2 has been demonstrated to induce cell type–specific changes in the expression of MMPs and TIMPs. In human dermal fibroblasts, RLN2 stimulates MMP1 expression but downregulates TIMP1 expression and reduces collagen deposition in the extracellular matrix (ECM) by reducing collagen secretion.[9] Relaxin positively regulates MMP1, MMP2, and MMP3 expression and inhibits TIMP1 expression in human lower uterine segment fibroblasts,[10] and in renal fibroblasts it induces ECM degradation by induction of MMP2 and MMP9.[17] In cultured hepatic stellate cells, RLN2 was reported to inhibit effective collagen deposition by decreased TIMP1 and TIMP2 secretion, and this contributed to reduction in rat liver fibrosis.[35] Importantly, MMPs and TIMPs are also associated with multiple functions during wound healing at the ocular surface, dry eye disease, corneal neovascularization, the development of corneal ulcera, and in pterygia.[42] MMP2 is expressed in the healthy cornea and upregulated during wound healing.[43] This indicates that MMP2 is an important factor in EMC turnover and remodeling of healthy and wounded cornea, especially in the subsequent phase of wound healing.[44] In the presence of rRLN2, elevated levels of MMP2 mRNA are expressed in the HCE cell line, revealing a novel rRLN2 action at the ocular surface potentially relevant during wound healing processes. MMP9 has been detected in the basal epithelial cell layer of the healing cornea and appears to play a role in the formation of the new epithelial lining after corneal wounding.[43] SC cells responded to rRLN2 with increased expression of MMP9, suggesting a potential paracrine role of secreted MMP9 in the tear fluid and the delivery of MMP9 via the ocular surface to the wounded area. MMP13 has been implicated in the renewal of epithelium at the wounded cornea since it is detectable only during wound healing.[43] Levels of MMP13 transcript remained unchanged in SC, HCjE, and HCE cells in the presence of rRLN2. Similar results have been reported for hepatic stellate cells, in which RLN2 was unable to alter MMP13 expression.[35] The interaction between TIMP1 and TIMP2 with MMP2 and MMP9 renders these MMPs inactive.[45] Intriguingly, longer exposure to rRLN2 increased TIMP1 and TIMP2 expression in cell lines derived from the ocular surface, and this delayed rRLN2-mediated secretion of TIMP1/2 may prevent disproportionate epithelial deposition.

The effects of rRLN2 on proliferation, migration, and MMP/TIMP expression derived from our in vitro cell models provide evidence for an intricate functional role of RLN2 at the ocular surface. Next, we determined the in vivo effects of RLN2 employing an in vivo corneal wound healing model. Intriguingly, RLN2 significantly increased the wound healing rate by markedly increasing re-epithelialization of the denuded corneal surface. These in vivo results emphasized the important novel role of RLN2 for maintenance and regeneration of the ocular epithelial cell layer.

These findings also identified for the first time a novel potential therapeutic application of RLN2. Local application of exogenous hrRLN2 is attractive because it is noninvasive and may provide a significant benefit to patients with corneal ulcerations of different origins and in the postoperative treatment of elective excimer laser surgery. Millions of these laser procedures are performed each year, and a delay in epithelial healing puts the cornea at risk of developing postoperative haze, infectious keratitis, and irreparable ulcerative corneal degradation and permanent visual impairment.

Acknowledgments

We thank Marlis Johne for the kind support, Ute Beyer and Susann Möschter for excellent technical assistance, Yvonne Radestock and Cuong Hoang-Vu for the kind supply of mRNA positive controls, Monica Berry for the kind support in fibroblast cultivation, and Claudia A. Krusche for support in RXFP1 primer creation.

References

1. Rieck PW, Pleyer U. [Corneal wound healing. II. Treatment of disorders of wound healing]. *Ophthalmologe*. 2003;100:1109–1130.
2. Hsu SY, Nakabayashi K, Nishi S, et al. Activation of orphan receptors by the hormone relaxin. *Science*. 2002;295:671–674.
3. Bathgate RA, Ivell R, Sanborn BM, Sherwood OD, Summers RJ. International Union of Pharmacology LVII: recommendations for the nomenclature of receptors for relaxin family peptides. *Pharmacol Rev*. 2006;58:7–31.
4. Kern A, Bryant-Greenwood GD. Mechanisms of relaxin receptor (LGR7/RXFP1) expression and function. *Ann N Y Acad Sci*. 2009;1160:60–66.
5. Vodstrcil LA, Wlodek ME, Parry LJ. Effects of uteroplacental restriction on the relaxin-family receptors, Lgr7 and Lgr8, in the uterus of late pregnant rats. *Reprod Fertil Dev*. 2007;19:530–538.
6. Lowndes K, Amano A, Yamamoto SY, Bryant-Greenwood GD. The human relaxin receptor (LGR7): expression in the fetal membranes and placenta. *Placenta*. 2006;27:610–618.
7. Dschietzig T, Bartsch C, Baumann G, Stangl K. Relaxin-a pleiotropic hormone and its emerging role for experimental and clinical therapeutics. *Pharmacol Ther*. 2006;112:38–56.
8. Dschietzig T, Richter C, Bartsch C, et al. The pregnancy hormone relaxin is a player in human heart failure. *FASEB J*. 2001;15:2187–2195.
9. Unemori EN, Amento EP. Relaxin modulates synthesis and secretion of procollagenase and collagen by human dermal fibroblasts. *J Biol Chem*. 1990;265:10681–10685.
10. Palejwala S, Stein DE, Weiss G, Monia BP, Tortoriello D, Goldsmith LT. Relaxin positively regulates matrix metalloproteinase expression in human lower uterine segment fibroblasts using a tyrosine kinase signaling pathway. *Endocrinology*. 2001;142:3405–3413.
11. Samuel CS, Lekgabe ED, Mookerjee I. The effects of relaxin on extracellular matrix remodeling in health and fibrotic disease. *Adv Exp Med Biol*. 2007;612:88–103.
12. Samuel CS, Mookerjee I, Halls ML, et al. Investigations into the inhibitory effects of relaxin on renal myofibroblast differentiation. *Ann N Y Acad Sci*. 2009;1160:294–299.
13. Silvertown JD, Summerlee AJ, Klonisch T. Relaxin-like peptides in cancer. *Int J Cancer*. 2003;107:513–519.
14. Lekgabe ED, Kiriazis H, Zhao C, et al. Relaxin reverses cardiac and renal fibrosis in spontaneously hypertensive rats. *Hypertension*. 2005;46:412–418.

Downloaded from iovs.arvojournals.org on 06/17/2019

15. Jeyabalan A, Novak J, Danielson LA, Kerchner LJ, Opett SL, Conrad KP. Essential role for vascular gelatinase activity in relaxin-induced renal vasodilation, hyperfiltration, and reduced myogenic reactivity of small arteries. *Circ Res*. 2003; 93:1249–1257.
16. Jeyabalan A, Shroff SG, Novak J, Conrad KP. The vascular actions of relaxin. *Adv Exp Med Biol*. 2007;612:65–87.
17. Heeg MH, Koziolek MJ, Vasko R, et al. The antifibrotic effects of relaxin in human renal fibroblasts are mediated in part by inhibition of the Smad2 pathway. *Kidney Int*. 2005;68:96–109.
18. Sullivan DA. Tearful relationships? Sex, hormones, the lacrimal gland, and aqueous-deficient dry eye. *Ocul Surf*. 2004;2:92–123.
19. The epidemiology of dry eye disease: report of the Epidemiology Subcommittee of the International Dry Eye WorkShop (2007). *Ocul Surf*. 2007;5:93–107.
20. Knop E, Knop N, Millar T, Obata H, Sullivan DA. The international workshop on meibomian gland dysfunction: report of the subcommittee on anatomy, physiology, and pathophysiology of the meibomian gland. *Invest Ophthalmol Vis Sci*. 2011;52:1938–1978.
21. Araki-Sasaki K, Ohashi Y, Sasabe T, et al. An SV40-immortalized human corneal epithelial cell line and its characterization. *Invest Ophthalmol Vis Sci*. 1995;36:614–621.
22. Diebold Y, Calonge M, Enriquez de Salamanca A, et al. Characterization of a spontaneously immortalized cell line (IOBA-NHC) from normal human conjunctiva. *Invest Ophthalmol Vis Sci*. 2003;44:4263–4274.
23. Zouboulis CC, Seltmann H, Neitzel H, Orfanos CE. Establishment and characterization of an immortalized human sebaceous gland cell line (SZ95). *J Invest Dermatol*. 1999;113: 1011–1020.
24. Pfaffl MW. A new mathematical model for relative quantification in real-time RT-PCR. *Nucleic Acids Res*. 2001;29:e45.
25. Paulsen FP, Woon CW, Varoga D, et al. Intestinal trefoil factor/TFF3 promotes re-epithelialization of corneal wounds. *J Biol Chem*. 2008;283:13418–13427.
26. Gunnersen JM, Fu P, Roche PJ, Tregear GW. Expression of human relaxin genes: characterization of a novel alternatively-spliced human relaxin mRNA species. *Mol Cell Endocrinol*. 1996;118:85–94.
27. Rocha EM, Cunha DA, Carneiro EM, Boschero AC, Saad MJ, Velloso LA. Identification of insulin in the tear film and insulin receptor and IGF-1 receptor on the human ocular surface. *Invest Ophthalmol Vis Sci*. 2002;43:963–967.
28. Bryant GD. The detection of relaxin in porcine, ovine and human plasma by radioimmunoassay. *Endocrinology*. 1972;91: 1113–1117.
29. Heringlake M, Heide C, Bahlmann L, et al. Effects of tilting and volume loading on plasma levels and urinary excretion of relaxin, NT-pro-ANP, and NT-pro-BNP in male volunteers. *J Appl Physiol*. 2004;97:173–179.
30. Steinetz BG, Brown JL, Roth TL, Czekala N. Relaxin concentrations in serum and urine of endangered species: correlations with physiologic events and use as a marker of pregnancy. *Ann N Y Acad Sci*. 2005;1041:367–378.
31. Harris LA, Steinetz BG, Bond JB, Lasano S, Swanson WF. Refinement of a commercial bench-top relaxin assay for pregnancy diagnosis using urine from domestic and nondomestic felids. *J Zoo Wildl Med*. 2008;39:170–179.
32. Bell RJ, Eddie LW, Lester AR, Wood EC, Johnston PD, Niall HD. Relaxin in human pregnancy serum measured with an homologous radioimmunoassay. *Obstet Gynecol*. 1987;69: 585–589.
33. Hombach-Klonisch S, Bialek J, Trojanowicz B, et al. Relaxin enhances the oncogenic potential of human thyroid carcinoma cells. *Am J Pathol*. 2006;169:617–632.
34. Samuel CS, Unemori EN, Mookerjee I, et al. Relaxin modulates cardiac fibroblast proliferation, differentiation, and collagen production and reverses cardiac fibrosis in vivo. *Endocrinology*. 2004;145:4125–4133.
35. Williams EJ, Benyon RC, Trim N, et al. Relaxin inhibits effective collagen deposition by cultured hepatic stellate cells and decreases rat liver fibrosis in vivo. *Gut*. 2001;49:577–583.
36. Binder C, Hagemann T, Husen B, Schulz M, Einspanier A. Relaxin enhances in-vitro invasiveness of breast cancer cell lines by up-regulation of matrix metalloproteases. *Mol Hum Reprod*. 2002;8:789–796.
37. Millar LK, Reiny R, Yamamoto SY, Okazaki K, Webster L, Bryant-Greenwood GD. Relaxin causes proliferation of human amniotic epithelium by stimulation of insulin-like growth factor-II. *Am J Obstet Gynecol*. 2003;188:234–241.
38. Radestock Y, Hoang-Vu C, Hombach-Klonisch S. Relaxin reduces xenograft tumour growth of human MDA-MB-231 breast cancer cells. *Breast Cancer Res*. 2008;10:R71.
39. Feng S, Agoulnik IU, Li Z, et al. Relaxin/RXFP1 signaling in prostate cancer progression. *Ann N Y Acad Sci*. 2009;1160: 379–380.
40. Wyatt TA, Sisson JH, Forget MA, Bennett RG, Hamel FG, Spurzem JR. Relaxin stimulates bronchial epithelial cell PKA activation, migration, and ciliary beating. *Exp Biol Med (Maywood)*. 2002;227:1047–1053.
41. Kamat AA, Feng S, Agoulnik IU, et al. The role of relaxin in endometrial cancer. *Cancer Biol Ther*. 2006;5:71–77.
42. Kim HS, Shang T, Chen Z, Pflugfelder SC, Li DQ. TGF-beta1 stimulates production of gelatinase (MMP-9), collagenases (MMP-1, –13) and stromelysins (MMP-3, -10, -11) by human corneal epithelial cells. *Exp Eye Res*. 2004;79:263–274.
43. Ye HQ, Maeda M, Yu FS, Azar DT. Differential expression of MT1-MMP (MMP-14) and collagenase III (MMP-13) genes in normal and wounded rat corneas. *Invest Ophthalmol Vis Sci*. 2000;41:2894–2899.
44. Azar DT, Hahn TW, Jain S, Yeh YC, Stetler-Stevensen WG. Matrix metalloproteinases are expressed during wound healing after excimer laser keratectomy. *Cornea*. 1996;15: 18–24.
45. Woessner JF Jr. The family of matrix metalloproteinases. *Ann N Y Acad Sci*. 1994;732:11–21.

Downloaded from iovs.arvojournals.org on 06/17/2019